Feasibility study of acoustic sensing for the welding pool mode in variable-polarity plasma arc welding

H Wang and **R Kovacevic***
Research Center for Advanced Manufacturing, Department of Mechanical Engineering,
Southern Methodist University, Richardson, Texas, USA

Abstract: The relationships between the acoustic signal and the modes of the welding pool, such as no-keyhole (melt-in), keyhole and cutting, in variable-polarity plasma arc welding are investigated. The Welch power spectral density (PSD) estimate and short-time Fourier transformation are implemented to analyse and identify the different modes of the welding pool. The results show that the no-keyhole mode (melt-in welding process) can be clearly distinguished from the keyhole and the cutting modes. The keyhole size is inversely proportional to the Welch PSD estimate of the acoustic signal.

Keywords: acoustic sensing, welding pool mode, variable-polarity plasma arc welding (VPPAW)

1 INTRODUCTION

Variable-polarity plasma arc welding (VPPAW) is a valuable arc welding process for aluminium alloys. In the keyhole mode VPPAW process, a high-energy-density high-velocity plasma jet is generated to melt and penetrate through the workpiece. The plasma jet momentum allows the jet to penetrate the welding pool completely to form a symmetric funnel-shaped cavity called a keyhole and a similarly shaped liquid–solid metal phase boundary. Metal fusion takes place when the molten metal flows around the keyhole and solidifies following jet passage. The VPPAW process has attractive capabilities such as the following:

(a) single-pass welding of $\frac{1}{2}$in (12.7 mm) aluminium alloy;
(b) 100 per cent joint penetration;
(c) consistent X-ray quality;
(d) minimal distortion;
(e) square groove preparation;
(f) reduced costs [1].

It has been used successfully in production, such as in the fabrication of the space shuttle external tanks and space station [**2**, **3**]. However, the keyhole welding pool is not very stable, and it can possibly turn into the melt-in (no-keyhole) process or the cutting process during welding. Thus, sensing and feedback control to ensure the stability of the keyhole welding pool remains a challenge.

The present sensing techniques for the stability of the welding pool or the weld penetration in keyhole plasma arc welding (PAW) can be divided into two classes according to the relative spatial location of the sensor and the workpiece: sensing from the back side of the workpiece (SFBS) and sensing from the front side of the workpiece (SFFS). SFBS includes mainly three sensing techniques:

1. *Sensing by the electrical conductivity of the plasma efflux* [**4**]. A metal bar is placed in the back side of the workpiece. After the plasma jet penetrates the workpiece, an electrically conductive passage can be established between the workpiece and the metal bar through the plasma efflux. Therefore, a detected change in voltage can be used to indicate the existence of a keyhole or full penetration.
2. *Sensing by sound signal in the welding process of a pipe* [**5**]. It is found that a sharp change in the sound signal can be detected when the keyhole exists. This sound signal includes a stable fundamental frequency of 300 Hz introduced by the fluctuation of the welding current.
3. *Sensing by light of the plasma efflux* [**6**, **7**]. The basic approach of this sensing technique is that a light signal of the plasma arc can be detected by a photocell fixed on the back side of the workpiece.

The SFBS techniques can meet a number of practical requirements. However, the SFBS techniques contribute

The MS was received on 18 February 2002 and was accepted after revision for publication on 24 June 2002.
**Corresponding author: Research Center for Advanced Manufacturing, Department of Mechanical Engineering, Southern Methodist University, 1500 International Parkway, Suite 100, Richardson, TX 75081, USA.*

to an access problem to the welding part with a closed structure, such as a tank. That access problem is why researchers pay more attention to the study of SFFS techniques.

SFFS includes mainly three sensing methods:

1. *Arc light sensing*. It is found that the keyhole mode can be detected by real-time spectroscopic measurements of the ratio of the hydrogen 656 nm line to the argon 696 nm line in VPPAW. This ratio decreases abruptly when the keyhole is established, presumably because the hydrogen is flushed out through the keyhole with the plasma jet. Unfortunately the cutting mode is difficult to identify from the keyhole mode by this approach because the hydrogen is also flushed out with the plasma jet [**8**]. By spectroscopic study of the plasma arc, information on the keyhole formation can be extracted in PAW [**9**]. The keyhole size cannot be detected precisely nor can the cutting mode be distinguished from the keyhole mode by this sensing technique.
2. *Sound sensing*. Sound sensing has been investigated in the PAW process. For example, the sound signal reflects the appearance and disappearance of the keyhole in the PAW of aluminium with direct current reverse polarity (DCRP). The sound signal could be used to control the start or stop of the welding carriage [**10**]. A workpiece with a variable thickness is used to generate the no-keyhole mode, transition mode and keyhole mode welding pool in the PAW process. It is found that the no-keyhole mode, transition mode and keyhole mode can be identified by the sound signal [**11**, **12**]. However, it remains in question whether the acoustic signal can be used to identify the cutting mode from the no-keyhole mode and keyhole mode. The cutting process is a basic mode and also a large problem in the PAW process. Until now, no literature on acoustic sensing in VPPAW has been reported.
3. *Image sensing*. The many advantages of image sensing include that it is intuitive, provides an abundance of information, has an absence of electromagnetic interference and is not intrusive. It was found in our previous research work that image sensing has a fairly good potential in monitoring the stability of the welding pool [**13**–**16**]. However, the field of view of the keyhole from the front side of the workpiece is very limited because the stand-off distance of the welding torch is only about 5.0 mm but the diameter of the welding torch is about 50.0 mm. The keyhole image cannot be detected effectively when the keyhole size is out of a specific range. This drawback limits the application of image sensing in VPPAW even though an improvement in the field of view of the keyhole has been made [**17**]. An additional sensing technique must be applied to assist the front-side image sensing to overcome its drawback. Acoustic sensing is one possible option. Therefore, this paper focuses on the investigation of the relationship between the acoustic signal signature and the welding pool mode in VPPAW.

2 EXPERIMENTAL PROCEDURES

The experimental set-up, as shown in Fig. 1, includes a variable-polarity welding power source, a computer-controlled positioning system, an optoelectronic detector, a free-field $\frac{1}{2}$ in microphone with a conditioning amplifier, and an analogue-to-digital converter–digital-to-analogue converter card. The distance between the microphone and the welding pool is about 86.0 mm, and the angle between the microphone and the axis of the torch is about 42°. As a reference, an optoelectronic detector is used to monitor the keyhole mode (no-keyhole, keyhole, cutting and so on) from the back side of the workpiece. The detection range of the acoustic signal is set up for the range from 0.1 Hz to 15 kHz. The acquisition of the acoustic signal and the acquisition of the optoelectronic signal are synchronized.

Six different experiments are designed as follows:

Experiment I. An aluminium alloy 5256 plate with the dimensions 76.2 mm × 178.0 mm × 4.8 mm, as shown in Fig. 2a, is used in the VPPAW process to study the effect of the welding pool mode (keyhole mode or no-keyhole mode) on the signature of the acoustic signal. Two holes with diameters of 3.57 and 4.37 mm are drilled into the plate along the welding line. The distance between them is 50.8 mm. The weld length is 152.4 mm, and the corresponding acoustic signal was acquired from 25.4 to 127.0 mm. The acquired acoustic signal is shown in Fig. 2b. A relatively low direct current electrode negative (DCEN) welding current of 60 A is applied to avoid melting the base metal and the two holes. Keeping the shapes of the drilled holes in good condition can help to distinguish precisely the difference between the acoustic signals of the no-hole mode and hole mode. The welding speed is 1.6 mm/s. Other welding

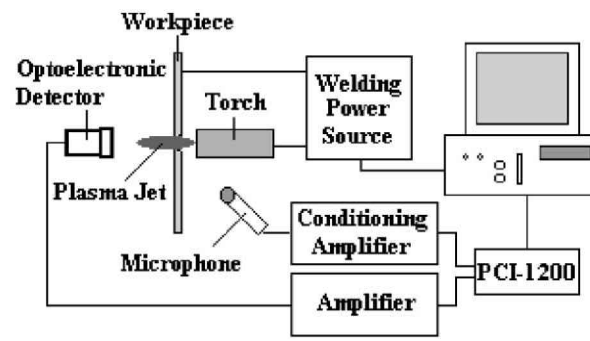

Fig. 1 Schematic diagram of the experimental set-up

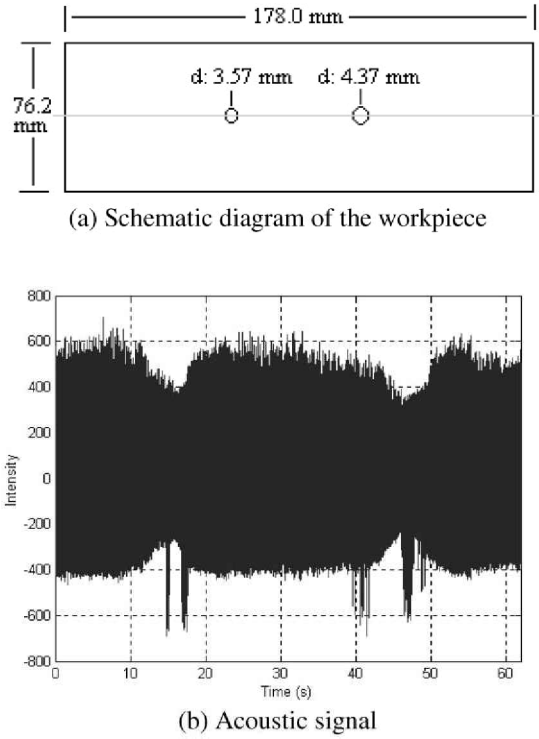

Fig. 2 Results of experiment I: simulating the welding process of a workpiece with pre-drilled holes

parameters are shown in Table 1. The signal acquisition frequency is 50 kHz.

Experiment II. An aluminium alloy 5256 plate with the dimensions 76.2 mm × 178.0 mm × 4.8 mm is used to study the effect of the welding pool mode on the signature of the acoustic signal in the real VPPAW process. In order to obtain two different welding pool modes (no-keyhole mode and keyhole mode) along one weld bead, the following procedure is used:

1. Step the DCEN welding current to 110 A without any sloping-up process at the beginning of welding process.
2. Start to move the workpiece at a normal welding speed without any delay at the beginning of welding process.

It takes a short time (usually less than 5 s) to establish a keyhole mode welding process. Therefore, in this case, there are two different phases in the welding process. In the first phase there is a no-keyhole mode, and in the second phase there is a keyhole mode. The total time span of the welding process is 78 s. The signal acquisition frequency is 30 kHz. The welding speed is 1.6 mm/s. Other welding parameters are shown in Table 1. The weld is shown in Figs 3a and b. The acquired acoustic signal and optoelectronic signal are shown in Fig. 3c.

Table 1 VPPAW parameters

Torch standoff	4 mm
Orifice diameter	3.57 mm
Throat length	3.175 mm
Electrode setback	2.0 mm
DCEN frequency	60 Hz
DCEP duty cycle	15 per cent
DCEP welding current	DCEN welding current × 160 per cent
Pilot arc current	15 A
Plasma gas flowrate	3.6 l/min
Shielding gas flowrate	9.5 l/min

Experiment III. The same kind of plate as that of experiment II is used to study the effect of the welding pool mode on the signature of the acoustic signal in the VPPAW process. Different welding speeds are applied to obtain two different welding pool modes (no-keyhole mode and keyhole mode) along the same weld bead. The length of the weld is 127.0 mm. In the first phase, 61.0 mm of a weld bead is welded with a relatively high welding speed of 7.62 mm/s. In the second phase, 66.0 mm of a weld bead is welded with a welding speed of 1.6 mm/s. The DCEN welding current is 110 A. The other welding parameters are shown in Table 1. The heat input depends on welding current, welding arc voltage and welding speed. When the welding current and the welding arc voltage are kept constant, the heat input decreases when increasing the welding speed. Therefore, the welding pool mode in the first phase is a no-keyhole mode because of low heat input. The welding pool mode in the second phase is a keyhole mode. The total time span of the welding process is 40 s: 8 s for the first phase, and 32 s for the second phase. The signal acquisition frequency is 30 kHz. The weld is shown in Figs 4a and b. The acquired acoustic signal and optoelectronic signal are shown in Fig. 4c.

Experiment IV. The heat-conducting condition is set to be asymmetric in order to obtain the different welding pool modes: no-keyhole mode and cutting mode. The same kind of plate as that of experiment II is used in this experiment. The purpose of this experiment is to study the effect of the cutting mode on the signature of the acoustic signal. Three steps are undertaken in this experiment:

1. Set workpiece holders very tightly on one side of the workpiece and relatively loosely on the other side.
2. Step the DCEN welding current to 110 A without any sloping-up process at the beginning of welding process.
3. Start to move the workpiece at a normal welding speed without any delay at the beginning of welding process.

It takes a short time to establish a keyhole in the workpiece; then the welding process changes into the cutting process because of the asymmetric heat-conducting condition. Thus, there are two different

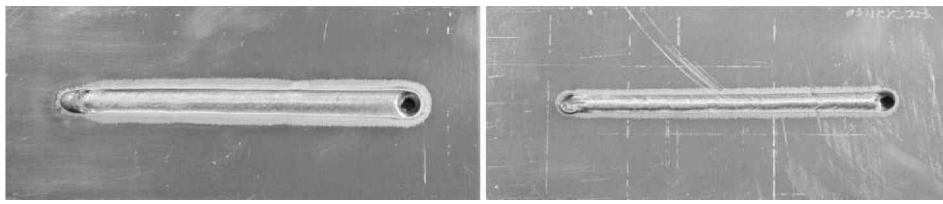

(a) Front-side photograph of workpiece **(b) Back-side photograph of workpiece**

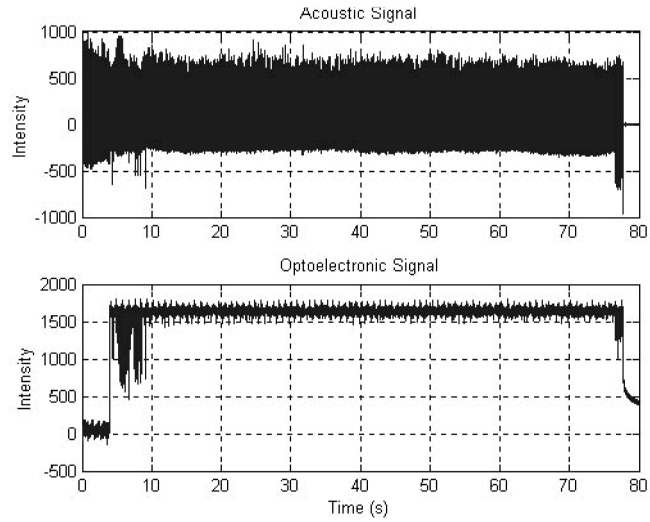

(c) Acquired signals

Fig. 3 Results of experiment II: normal VPPAW process

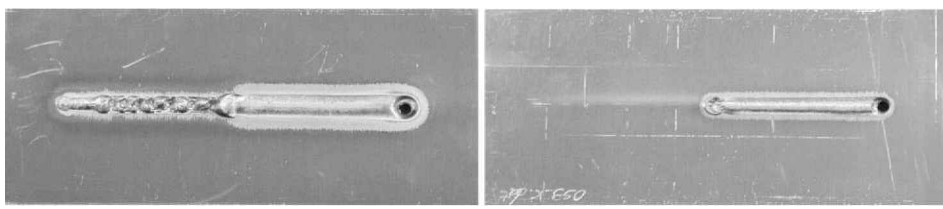

(a) Front-side photograph of workpiece **(b) Back-side photograph of workpiece**

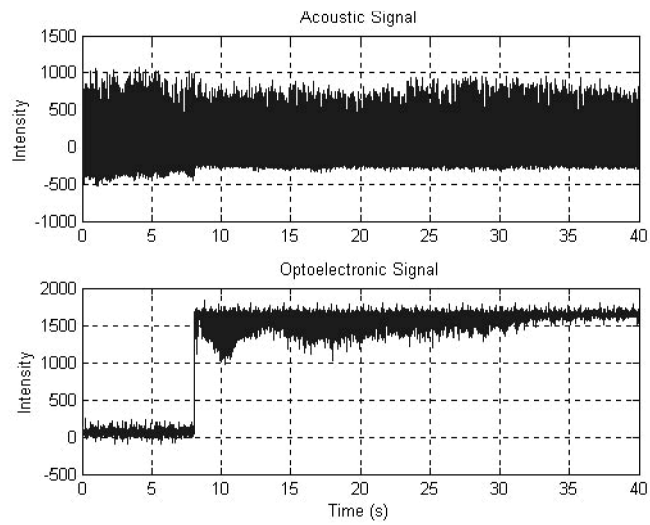

(c) Acquired signals

Fig. 4 Results of experiment III: VPPAW process with a variable welding speed

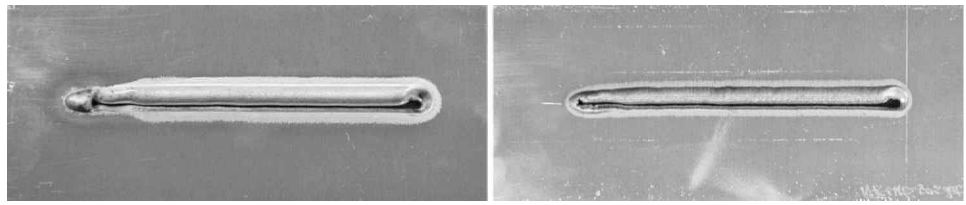

(a) Front-side photograph of workpiece **(b) Back-side photograph of workpiece**

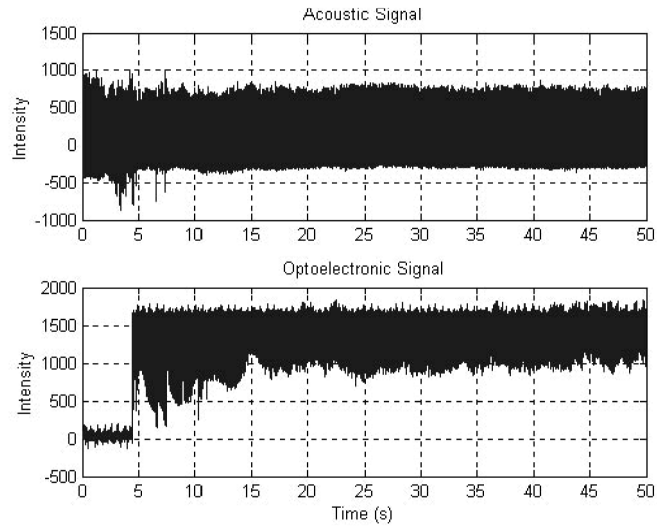

(c) Acquired signals

Fig. 5 Results of experiment IV: cutting process with variable heat conduction

welding pool modes in the welding process. The welding pool mode is a no-keyhole mode in the first phase and a cutting mode in the second phase. Acoustic and optoelectronic signals are acquired during the first 50 s of the welding process. The signal acquisition frequency is 30 kHz. The welding speed is 1.6 mm/s. Other welding parameters are shown in Table 1. The weld is shown in Figs 5a and b. The acquired acoustic signal and optoelectronic signal are shown in Fig. 5c.

Experiment V. A specially prepared workpiece with a variable heat sink is used to obtain different sizes of keyhole during the welding process. As shown in Fig. 6a, two narrow slits are made to change the heat sink on the aluminium alloy 5256 plate with the dimensions 76.2 mm × 178.0 mm × 4.8 mm. The purpose of this experiment is to study the effect of the keyhole size on the signature of the acoustic signal. The welding speed is 1.6 mm/s. The DCEN welding current is 110 A. Other welding parameters are shown in Table 1. The total time span of the welding process is 76 s. The signal acquisition frequency is 30 kHz. There are two welding pool modes in the welding process: no-keyhole mode and keyhole mode. The acquired acoustic signal and optoelectronic signal are shown in Fig. 6c.

Experiment VI. A specially prepared workpiece with a variable heat sink and a pre-drilled hole is applied to obtain a normal welding process and a cutting process in one pass. By pre-drilling a hole (diameter, 5.0 mm) in the path of the weld, cutting is generated at the position of the pre-drilled hole because there is not enough molten metal in the welding pool and because a variable heat sink is present. Except for the pre-drilled hole, the workpiece has the same dimensions and material property as the workpiece in experiment V. The purpose of this experiment is to study whether the acoustic signal can be used to distinguish the cutting mode from the keyhole mode. The welding speed is 1.6 mm/s. The DCEN welding current is 110 A. Other welding parameters are shown in Table 1. The time span of the welding process is 75 s. The signal acquisition frequency is 30 kHz. The weld is shown in Figs 7a and b. The acquired acoustic signal and optoelectronic signal are shown in Fig. 7c.

3 ACOUSTIC SIGNAL ANALYSES

3.1 Analysis of the acoustic signal in the time domain

It is seen, from the result of experiment I, that the mode of the simulated welding pool (with a pre-drilled hole) has an obvious effect on the acquired acoustic signal. As shown in Fig. 2b, the intensity of the acoustic signal in the 'no-keyhole' mode (without a pre-drilled hole) is

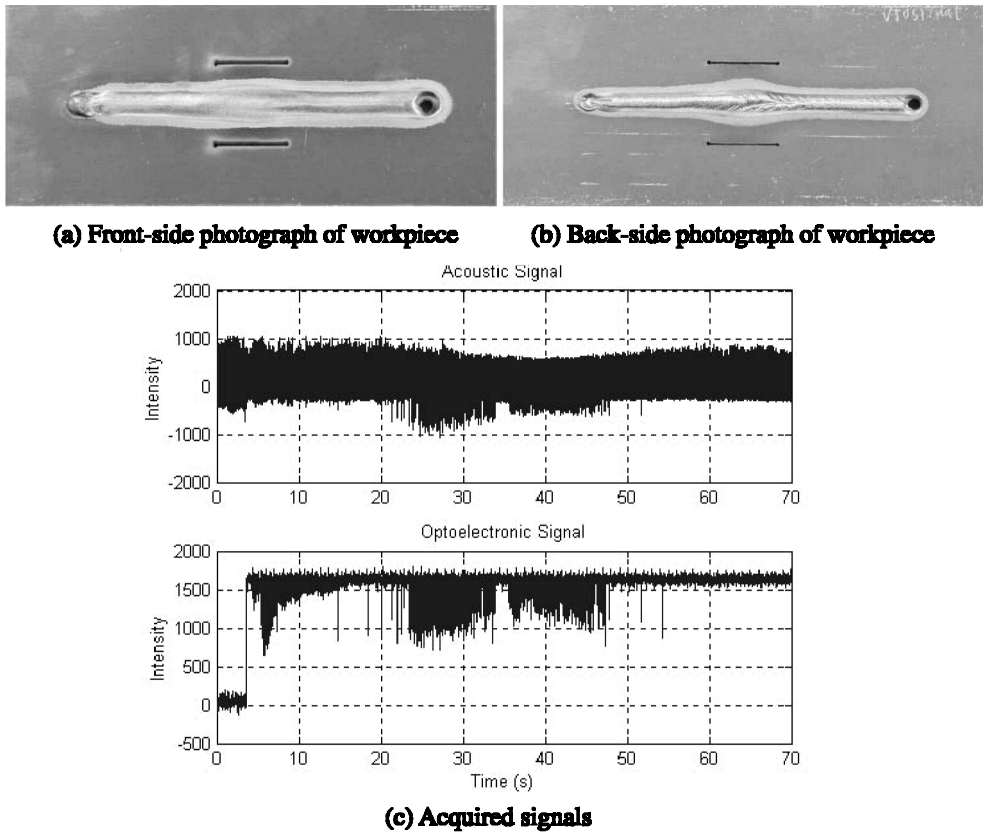

(a) Front-side photograph of workpiece (b) Back-side photograph of workpiece

(c) Acquired signals

Fig. 6 Results of experiment V: VPPAW process with a variable heat sink

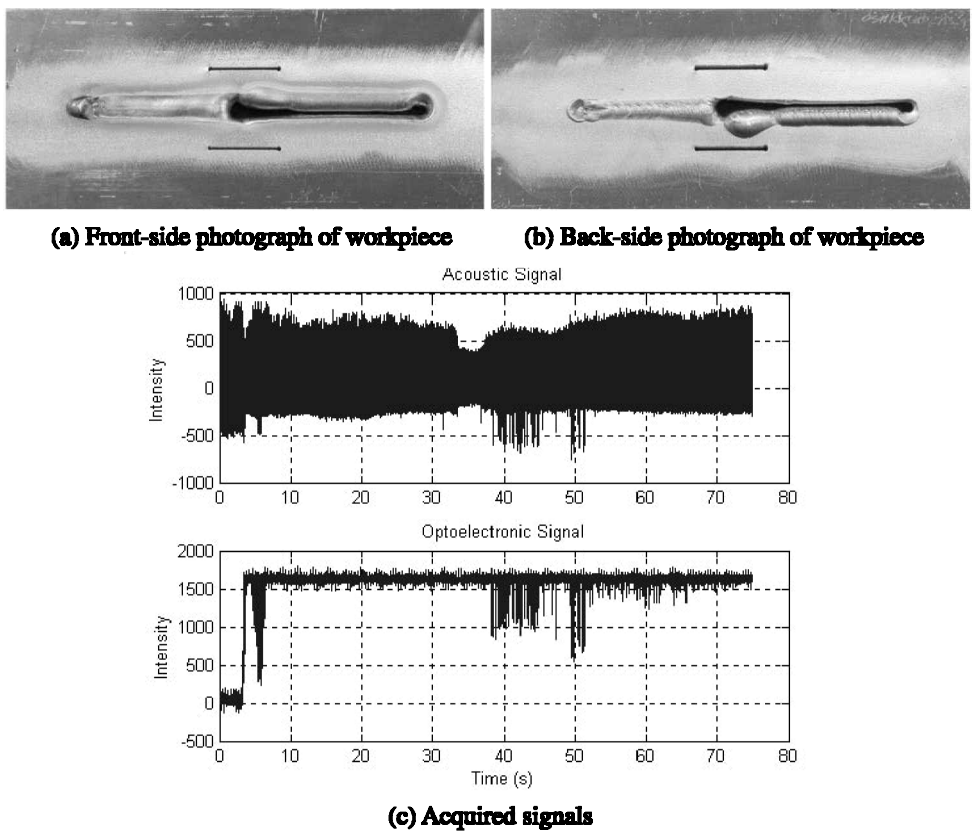

(a) Front-side photograph of workpiece (b) Back-side photograph of workpiece

(c) Acquired signals

Fig. 7 Results of experiment VI: VPPAW process with a pre-drilled hole and a variable heat sink

higher than that in the 'keyhole' mode (with a pre-drilled hole). The intensity of the acoustic signal found with a smaller diameter of a pre-drilled hole (3.57 mm) is relatively higher than that signal found with a larger diameter of a pre-drilled hole (4.37 mm). It appears that the intensity of the acoustic signal is *inversely* proportional to the size of the pre-drilled hole.

A possible mechanism for this phenomenon can be described as follows: the intensity of the acoustic signal can be measured as a function of the sound pressure change. The relation between the intensity I of the acoustic signal and the sound pressure P can be described by the following equation:

$$I = \frac{P^2}{\rho c} \quad \mathrm{W/m^2} \tag{1}$$

where ρ (=1.21 kg/m^2) and c (=344 m/s) are the density of air and the velocity of sound respectively. Therefore, the variation in the sound pressure P results in a different intensity of the acoustic signal. Assuming that the welding parameters are constant in the VPPAW process, the sound pressure P generated by the plasma arc decreases at the position where the pre-drilled hole exists because of the pressure leaking through the hole. The larger the pre-drilled hole diameter, the greater is the loss of the sound pressure, and the lower is the intensity of the acoustic signal acquired by the microphone in front of the workpiece.

The details of the acoustic signal acquired in experiment I are shown in Fig. 8. It is seen that the acoustic signal clearly reflects the polarity change of the welding current. The VPPAW waveform is shown in Fig. 9,

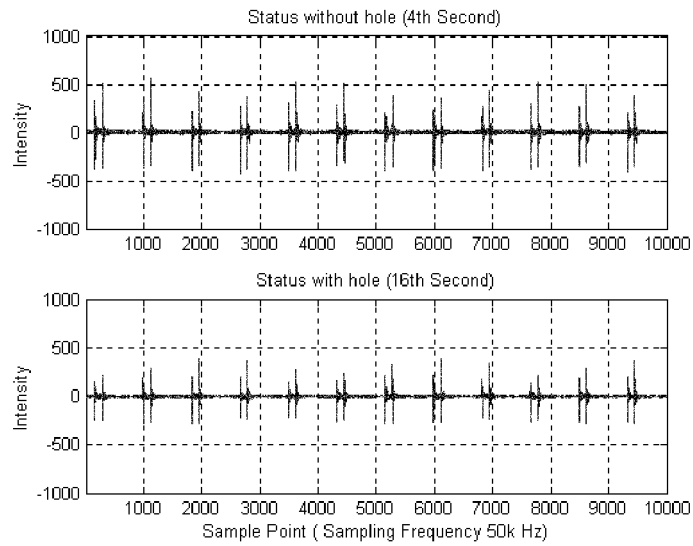

(a) 10,000 sampling points

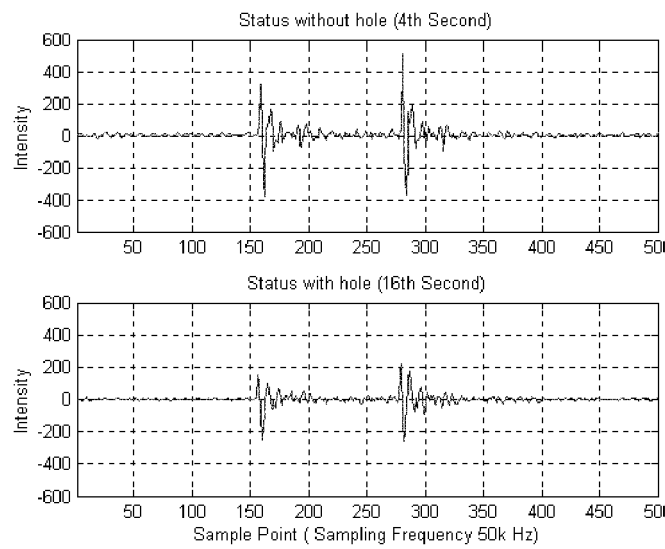

(b) 500 sampling points

Fig. 8 Intensity comparison of the acoustic signal with respect to the existence of the pre-drilled hole

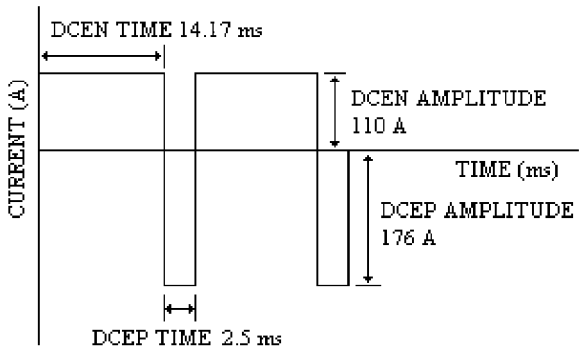

Fig. 9 VPPAW current waveform

where DCEN means that a dc with the electrode is connected to the negative, and DCEP means that a dc with the electrode is connected to the positive. It is seen in Fig. 8 that the acoustic signal is periodic. The periodic time of the acoustic signal is equal to that of the VPPAW current. In a period, there are two high amplitudes that occur at the instant that the polarity changes. The high amplitudes are followed by damped waves, as shown in Fig. 8b. The maximum amplitude usually takes place at the instant that the polarity changes from DCEP to DCEN. The intensity of the acoustic signal slightly fluctuates at different periods.

The details of the acoustic signal acquired in experiment II, a real VPPAW process, are shown in Fig. 10. It can be seen that the acoustic signal has the same characteristics as those obtained in experiment I. The intensity of the acquired signal is higher than that in experiment I. The reason is that the amplitudes of the welding current are different in experiment I (60 A) and experiment II (110 A).

Results from experiments II to VI can be summarized as follows:

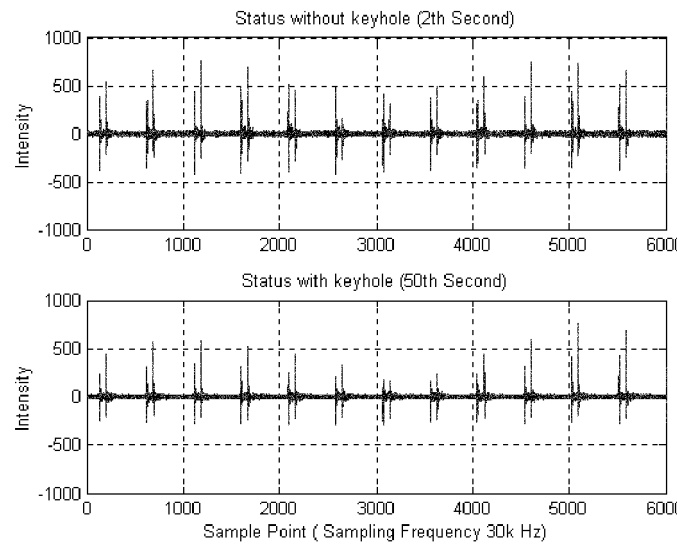

(a) 6000 sampling points

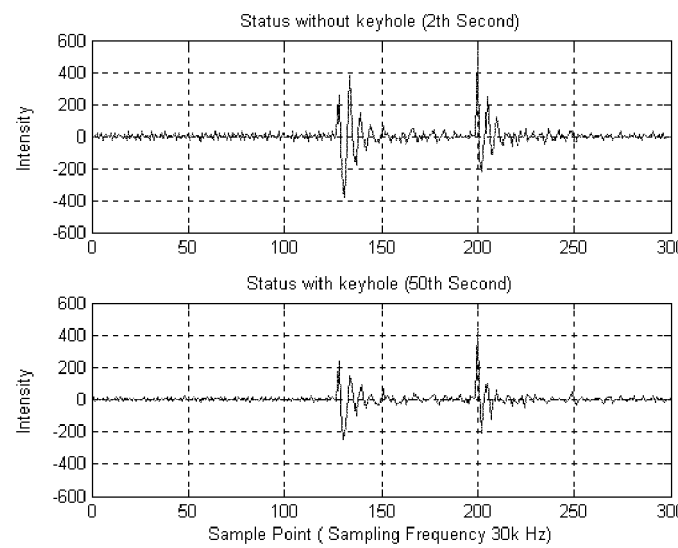

(b) 300 sampling points

Fig. 10 Intensity comparison of the acoustic signal with respect to the existence of the keyhole

1. The results of experiments II, III, V and VI, as shown in Fig. 3, Fig. 4, Fig. 6 and Fig. 7 respectively, demonstrate that the intensity of the acoustic signal before the keyhole is established is higher than the intensity after the keyhole occurs. However, the trend is not so obvious and it is still difficult to distinguish between the no-keyhole mode and keyhole mode based on the raw acoustic signal.
2. The result of experiment IV, as shown in Fig. 5, also demonstrates that the intensity of the acoustic signal before the keyhole is established is higher than that when cutting occurs. By comparing the results of experiment II (normal keyhole welding process) and experiment IV (cutting process), it can be seen that it is very difficult to distinguish between the two different processes by observing the unprocessed acoustic signal.
3. The result of experiment V, as shown in Fig. 6, demonstrates that the positive part of the intensity of the acoustic signal can reflect a trend in the change in the keyhole size.
4. The transition from a no-keyhole mode to a keyhole mode or from a no-keyhole mode to a cutting mode is very short according to the acquired optoelectrical signal.
5. The acoustic signal is stable during the keyhole welding process or the cutting process.
6. The acoustic signal is positively biased.

3.2 Identification of the no-keyhole mode

The goal of spectral estimation is to describe the distribution (over frequency) of the power of a signal based on a finite set of data. An improved estimator of the power spectral density (PSD) is that proposed by Welch [**18**]. The algorithm is as follows:

1. The input signal vector $\boldsymbol{x}$ is divided into k overlapping segments. The number of segments, k, that $\boldsymbol{x}$ is divided into is calculated as

$$k = \frac{m - o}{l - o} \tag{2}$$

where m is the length of the signal vector $\boldsymbol{x}$, o is the number of overlapping samples and l is the length of each segment (the window length).

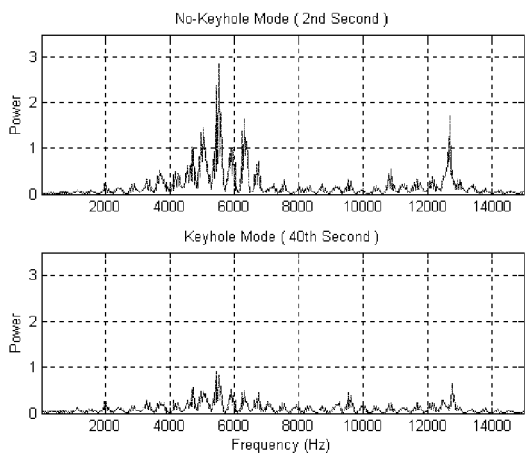

(a) Normal VPPA welding process

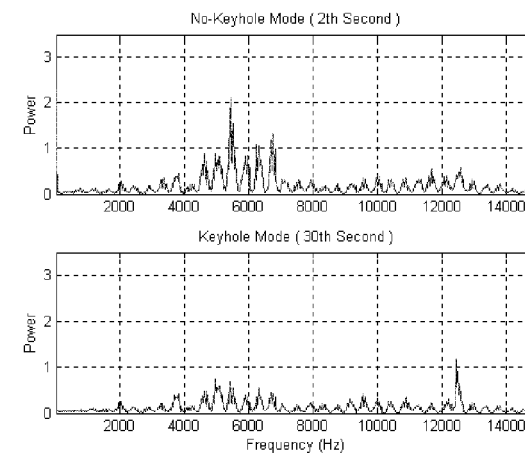

(b) Variable welding speed VPPA welding process

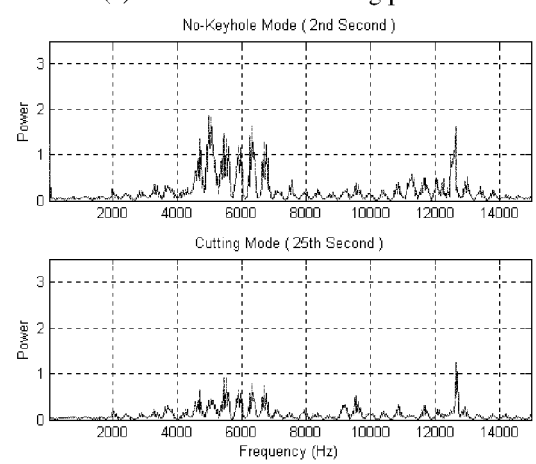

(c) Cutting process with variable heat conduction

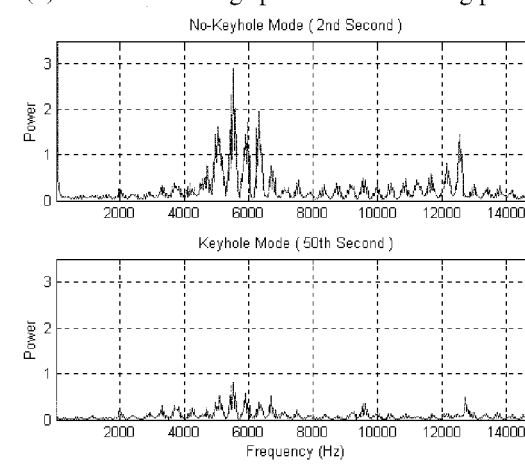

(d) VPPA welding process with variable heat sink

Fig. 11 Comparison results of different keyhole modes based on the Welch PSD estimate

2. The specified window (e.g. the Hanning window) is applied to each segment of $\boldsymbol{x}$.
3. A 1024-point fast Fourier transform is applied to the windowed data.
4. The modified periodogram of each windowed segment is computed.
5. The set of modified periodograms is averaged to form the spectrum estimate $S(e^{j\omega})$.
6. The resulting spectrum estimate is scaled to compute the PSD as $S(e^{j\omega})/f_s$, where f_s is the sampling frequency.

In order to analyse the difference between the Welch PSD estimates of the acoustic signals of the different welding pool modes, data are selected from different processes such as the no-keyhole process, keyhole process and cutting process in experiments II, III, IV and V and then processed with the Welch PSD estimate. The results are shown in Fig. 11. In general, all the experiment results show that the acoustic signal has a higher power amplitude in the no-keyhole mode than in the keyhole mode or cutting mode. The sharp difference in power amplitude occurs in two frequency ranges: 4500–7000 Hz and 11 000–13 000 Hz.

An algorithm is designed to identify the keyhole mode based on the Welch PSD estimate. Firstly, the acquired data are divided into small data sections with equal lengths denoted DL. Assuming that $P_{xx}(f)$ is the results of the Welch PSD estimate, then an integration of $P_{xx}(f)$ from 4500 to 7000 Hz is applied as follows:

$$P(k) = \sum_{f=4500}^{7000} P_{xx}(f) \tag{3}$$

where f is the frequency, $k = 1, 2, \ldots,$ COUNT/DL. COUNT is the length of the acquired data. The results of $P(k)$ for the different experiments are shown in Fig. 12. DL is equal to 15 000, and the sampling frequency is 30 kHz. Therefore two calculated results can be obtained per second. It can be found that the no-keyhole mode can be distinguished clearly from the keyhole mode and cutting mode. For example, if the threshold is set to 40, the no-keyhole mode can be distinguished from the

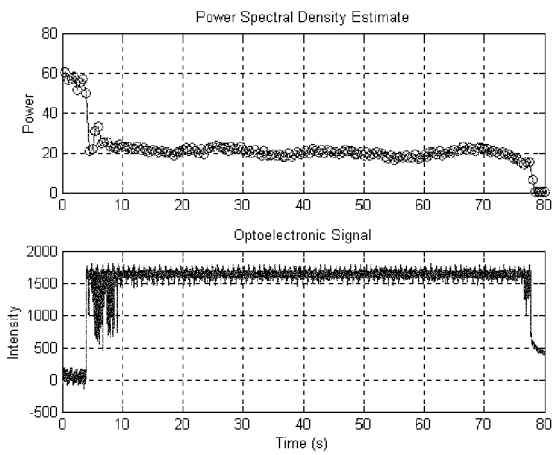

(a) Normal VPPA welding process

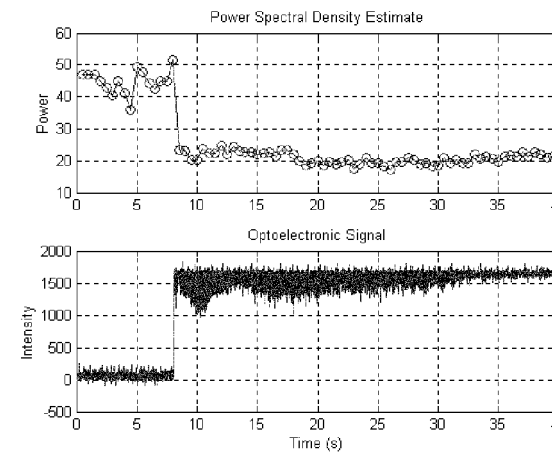

(b) Variable welding speed VPPA welding process

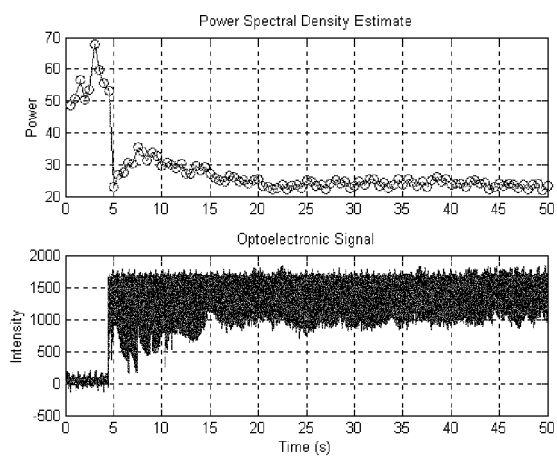

(c) Cutting process with variable heat conduction

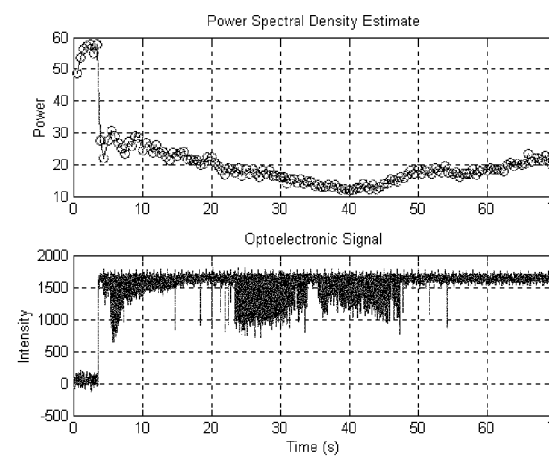

(d) VPPA welding process with variable heat sink

Fig. 12 Identification results of the no-keyhole mode

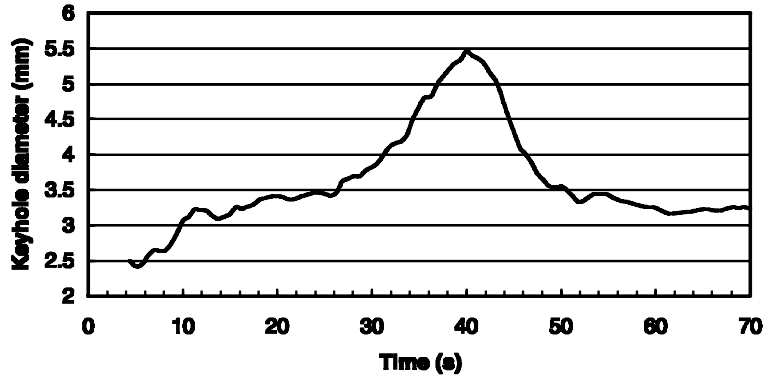

Fig. 13 Size variation of the keyhole in the experiment with a workpiece of variable heat sink

keyhole mode or cutting mode in experiments II, IV and V. The result of experiment III is an exception because of the main welding parameter where the welding speed is five times the normal welding speed in the first phase of the welding process. Therefore, there is a larger fluctuation in the processed results. However, the no-keyhole mode can still be distinguished from the keyhole mode by setting the threshold between 27 and 35. It can also be seen that it is difficult to distinguish the cutting mode from the keyhole mode by $P_{xx}(f)$ or $P(k)$ directly.

The keyhole diameter in experiment V is measured after the welding process has been carried out, and the result is shown in Fig. 13. By comparing the result with Fig. 12d, it can be concluded that the result of the Welch PSD estimate can reflect a trend in the change in the keyhole size. The keyhole size is inversely proportional to the Welch PSD estimate result of the acoustic signal. This phenomenon verifies, again, that the intensity of the acoustic signal is inversely proportional to the keyhole size.

3.3 Discussion on the identification of cutting mode

Figure 14 shows the identification results of the welding pool modes in experiment VI based on the Welch PSD estimate. By comparing the result with Fig. 12d, it can be concluded that the cutting mode could not be distinguished from the keyhole mode by the Welch PSD estimate. The reason lies in the fact that both the keyhole mode and the cutting mode of the welding pool can result in a loss of part of the sound pressure generated by the plasma jet. In order to study the difference between the signatures of the acoustic signals of the keyhole mode and cutting mode, a short-time Fourier transformation is used to process the acoustic signal acquired in experiment VI. However, it shows that no marked difference can be found in the areas corresponding to the keyhole welding process and the cutting process. A small difference can be found around a frequency of 12 500 Hz. The intensity of the acoustic signal is slightly higher in the keyhole welding process

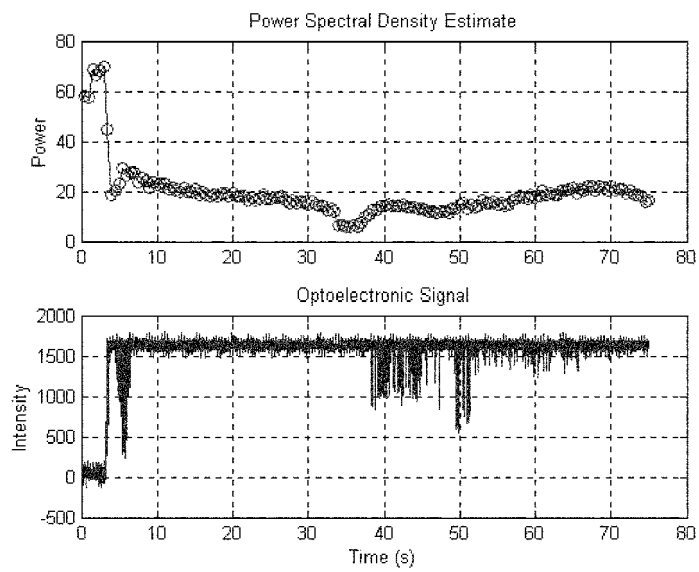

Fig. 14 Identification result of the keyhole mode and the cutting mode

than in the cutting process, but this difference is inadequate to use to identify the cutting mode. This is a shortcoming of acoustic sensing in keyhole VPPAW.

4 CONCLUSION

The acoustic signal is biased and clearly reflects the polarity change of the welding current in VPPAW. High amplitudes occur at the instant of polarity change. The high amplitudes are followed by damped waves. The transition from the no-keyhole mode to the keyhole mode or from the no-keyhole mode to the cutting mode is very short. There is a general trend that the intensity of the acoustic signal is higher before the keyhole is established than when the keyhole or the cutting mode occurs. However, noises and amplitude fluctuation of the acoustic signal always exist and the trend is not very obvious. Therefore, it is still difficult to distinguish the no-keyhole mode from the keyhole mode or the cutting mode directly from the original acoustic signal. By using the Welch PSD estimate, the no-keyhole mode can be clearly distinguished from the keyhole mode or the cutting mode. The keyhole size is inversely proportional to the Welch PSD estimate of the acoustic signal because much more sound pressure generated by the plasma jet leaks through the keyhole with a larger size. No adequate information in the time domain, frequency domain or time–frequency domain can be extracted to distinguish the cutting mode from the keyhole mode in the experimental conditions used in this paper. Although it is not a perfect monitoring approach for the welding pool mode, acoustic sensing still provides valuable assistance for front-side image sensing in keyhole VPPAW. To accomplish a good keyhole welding process, both the cutting and the melt-in (no-keyhole) processes should be avoided. Acoustic sensing is very useful to avoid the melt-in process. Acoustic sensing can precisely distinguish whether the keyhole is established or not and reflects the keyhole size. This is very useful when the keyhole size is very small or very large and out of the monitoring range of the image sensor.

ACKNOWLEDGEMENTS

This work was financially supported by National Science Foundation Grant DMI-9900011, by the US Department of Education Grant P200A80806-98 and by the Brown Foundation.

REFERENCES

1 **Craig, E.** The plasma arc process—a review. *Weld. J.*, 1988, **2**, 19-s–25-s.

2 **Nunes, A. C.** Variable polarity plasma arc welding on space shuttle external tank. *Weld. J.*, 1984, **63**(4), 27-s–35-s.

3 **Woodward, A. H.** U.S. contractor for the International Space Station. *Weld. J.*, 1996, **3**, 35-s–40-s.

4 **Steffens, H. D.** Automatic control for plasma arc welding with constant keyhole. *Weld. J.*, 1972, **6**, 40–45.

5 **Hu, B. X.** Study of quality control system of pulsed plasma arc all-position welding by sound signal. *HanJie* (*China*), 1980, **3**, 17–20.

6 **Chi, Y. K.** Penetration quality closed-loop control in pulsed plasma arc welding. *Trans. Weld.* (*China*), 1980, **7**(1), 11–16.

7 **Inoue, K.** and **He, D.-F.** Penetration-self-adaptive free-frequency pulsed plasma arc welding process control with photocell sensor. *Trans. Japan Weld. Res. Inst.*, 1984, **13**(1), 2–6.

8 **Martinez, L. F., Marques, R. E., McClure, J. C.** and **Nunes, A. C.** Front side keyhole detection in aluminum alloys. *Weld. J.*, May 1992, 49–52.

9 **Dong, C., Zhu, Y., Zhang, H., Shao, Y.** and **Wu, L.** Study on front side arc light sensing in keyhole mode plasma arc welding. *Jixie Gongcheng Xuebao* (*Chin. J. Mech. Engng*), March 2001, **37**(3), 30–33.

10 **Zhang, J. H., Wang, Q. L., Cui, H. J.** and **Yin, S. Y.** Study on arc sound in TIG and plasma welding processes and the possibility of its application in practice. In Proceedings of the International Conference on *Quality and Reliability in Welding*, Hangzhou, PR China, 1984, pp. D.33.1–D.33.6.

11 **Wang, Y. W., Chen, Q., Sun, Z. G., Sun, J. W.** and **Wang, H. Y.** Sound sensing of the keyhole behaviors in plasma arc welding. *Jixie Gongcheng Xuebao* (*Chin. J. Mech. Engng*), January 2001, **37**(1), 53–56.

12 **Wang, Y. W., Chen, Q., Sun, Z. G.** and **Sun, J. W.** Relationship between sound signal and weld pool status in plasma arc welding. *Trans. Nonferrous Metals Soc. China*, February 2001, **11**(1), 54–57.

13 **Zheng, B., Wang, H. J., Wang, Q. L.** and **Kovacevic, R.** Imaging the keyhole in PAW of aluminum alloys. *Trans. ASME, J. Mfg Sci. Engng*, 1999, **121**(3), 372–377.

14 **Wang, H., Kovacevic, R., Zheng, B.** and **Wang, Q.** Real-time image processing of keyhole puddle in variable polarity plasma arc welding. *Proc. Instn Mech. Engrs, Part B, Journal of Engineering Manufacture*, 2000, **214**(B6), 495–504.

15 **Zheng, B., Wang, H. J., Wang, Q. L.** and **Kovacevic, R.** Control for weld penetration in VPPAW of aluminum alloys using the front weld pool image signal. *Weld. J.*, December 2000, **79**(12), 363-s–371-s.

16 **Liu, Z. H.** and **Wang, Q. L.** Edge detection and automatic threshold based on wavelet transform in the VPPAW keyhole image processing. In Proceedings of the IAS Annual Meeting (IEEE Industry Applications Society), Vol. 2, 35th IAS Annual Meeting and World Conference on *Industrial Applications of Electrical Energy*, Rome, Italy, 8–12 October 2000, pp. 1048–1053.

17 **Wang, H.** and **Kovacevic, R.** Keyhole Image Sensing in VPPAW. In Proceedings of the 7th Mechatronics Forum International Conference, Atlanta, Georgia, 6–8 September 2000.

18 **Welch, P.D.** The use of fast Fourier transform for the estimation of power spectra: a method based on time averaging over short, modified periodograms. *IEEE Trans. Audio Electroacoust.*, June 1967, **AU-15**(2), 70–73.